

FLEXURAL ANALYSIS OF STEEL MESH REINFORCED POLYURETHANE CONCRETE MATERIAL

Dandan Hu¹, Liangxiang Guo² and Baozhen Yan³

- 1. School of Civil and Architectural Engineering, Harbin University, No.109 Zhongxing Road, Harbin, Heilongjiang Province, China; Hardandan@163.com*
- 2. Construction Department, Guangzhou Highway Engineering Group Co. LTD, No. 6 Suiyin Erheng Road, Guanzhou, Guangdong Province, China*
- 3. Design Department, Heilongjiang Province Highway Bridge Survey Design Co. Ltd., No. 90 Qingbin Road, Harbin, Heilongjiang Province, China*

Received: 07.10.2024

Received in revised form: 16.12.2024

Accepted: 15.01.2025

ABSTRACT

In this paper, a new method of steel mesh reinforced polyurethane concrete (SMPC) material for bridge reinforcement is proposed because of the peeling failure of the reinforced layer of steel mesh reinforced polymer mortar (SMPM) material. Using the excellent anti-corrosion and tensile properties of high-strength steel mesh, as well as the advantages of strong adhesion and fast curing speed of polyurethane concrete, the two materials are combined together. In order to verify the feasibility of this strengthening method, the mechanical properties of SMPC material are investigated by bending test of SMPC material sheet. The main factors affecting the tensile properties of the composites are analyzed by considering the test variables such as specimen width, specimen thickness, glue-powder ratio and curing time. Based on the simplified tension model of high strength steel wires and the stress-strain relationship between tension and compression of polyurethane concrete, the calculation method of flexural bearing capacity of composite materials is obtained. The test results show that the flexural strength of the composite can be improved by increasing the width of the specimen, and the deflection can be reduced by increasing the reinforcement ratio, while the influence of the glue-powder ratio on the deflection is small.

KEYWORDS

Steel mesh reinforced polyurethane concrete (SMPC) material, Steel mesh reinforced polymer mortar (SMPM) material, Flexural performance test, Analysis of influence factors

INTRODUCTION

With the increase of bridge operation time and vehicle load, the structural diseases of bridge are increasing. For bridges with structural diseases, their bearing capacity and structural durability may not meet the requirements of the current code. There are big security risks, demolition and reconstruction is not economical and unreasonable. The existing old bridges are tested and evaluated, and reinforced and reformed according to the actual situation of the bridges [1-3]. This

can not only increase the life of the old bridge in service, but also save a lot of costs, bring huge economic benefits to the society, and reduce the occurrence of bridge accidents [4-6].

The steel mesh has the characteristics of light weight and high strength, and composite mortar is often used as the bonding and anchoring material. The composite mortar and steel mesh is used to strengthen the bridge structure. Xing [7] conducted an experimental study on the flexural performance of reinforced concrete beams reinforced by steel mesh reinforced polymer mortar (SMPM) material, and the results showed that the reinforcement of reinforced concrete beams by PM-SWM was an effective means of flexural reinforcement. Compared with the contrast beam, the bearing capacity and stiffness of the reinforced beam are significantly improved, and the calculation method of the flexural bearing capacity of the reinforced beam is proposed. Wang [8] conducted a test study on the shear resistance of reinforced concrete (RC) beams reinforced by high-strength steel mesh and polymer mortar. The damage mode, load-deflection curve, strength, stiffness and ductility of the beam are studied and analyzed. The mechanical properties of the reinforced beams are improved, and the shear resistance is increased by 38.47% ~ 71.37%. Finally, according to the specification, the prediction model of the shear capacity of the test beam is established. However, due to the poor tensile property and bonding property of the composite mortar, the SMPM reinforcement layer will be stripped and damaged, and the utilization rate of the steel stranding network will be reduced [9-13].

Polyurethane concrete (PC) material not only has fast setting speed and high early strength, but also shows the advantages of light weight, high strength and high toughness after curing. The material itself has good bonding strength and acid and alkali corrosion resistance [14-17]. Polyurethane concrete (PC) composite material is gradually applied in the field of bridge reinforcement. PC material is a new type of composite material with polyurethane as matrix and cement as reinforcement, which has the advantages of corrosion resistance, light weight and high strength. Zhang [18] conducted an experimental study on reinforced concrete T-beams reinforced by SMPC material. Factors such as the rate of wire mesh placement and the type of material the wire mesh is embedded in are considered. The test results show that SMPC reinforced beams exhibit greater yield load, ultimate load and stiffness than PM-SWM reinforced beams, and SMPC material reinforced beams can effectively inhibit crack propagation. Zhang [19] conducted a study on the flexural performance of reinforced concrete T-beams reinforced by SMPC material, and the test results showed that SMPC materials could significantly improve the flexural bearing capacity of the reinforced beams. Compared with the beams reinforced by PM-SWM, the beams reinforced by SMPC materials did not have peeling damage, and it can inhibit the generation and development of cracks.

In order to further apply SMPC material to practical engineering, it is necessary to further study the flexural properties of the composites. The four-point flexural test of thin plate specimens is carried out, and the failure mode and characteristics of thin plate specimens under load are investigated. Based on the simplified tensile model of steel mesh and the PC stress-strain relationship, the calculation method of flexural bearing capacity of composites is obtained, which provides a basis for material design and engineering application of urethane cement-steel mesh composites.

TESTING PROGRAM

Specimen design and preparation

The four-point bending test of SMPC material plate with length of 400 mm was carried out. The thickness of the thin-plate specimens is 25 mm. The wire mesh is welded by high-strength steel wire with a diameter of 1mm, and the square hole size of the wire mesh is 15 mm×15 mm.

The variables considered in the four-point bending test are the thickness of the specimen and the ratio of polyurethane to cement powder. Specimen widths are 120 mm, 100 mm, 80 mm and 60

mm, respectively. The weight of rubber powder in polyurethane concrete is 0.5, 1.0 and 1.5, respectively. A total of 3 specimen sets and 12 specimen groups (3 specimens in each group) were designed and produced, with a total of 36 thin-plate specimens. The F-a specimen set consists of 4 specimen groups, including F-a1, F-a2, F-a3 and F-a4. Each specimen group has a different width to explore the influence of specimen width on the bending properties of thin-plate specimens. The F-b set is similar to the F-a set, each containing four test sets, and only the PU cement mix ratio is changed to explore the influence of PU cement powder ratio on the bending properties of the composite. F-c sets were used as variables for 4 groups of steel mesh with different layers, and the influence of steel mesh reinforcement ratio on the bending performance of the sheet was investigated. Detailed design parameters of thin plate specimens are shown in Table 1.

Tab. 1 - Design parameters of thin plate specimens

Specimen set	Specimen group	Steel mesh layers	PC mix ratio	Specimen width/mm	Longitudinal wire spacing/mm
F-a	F-a 1	4	0.5	120	45
	F-a 2	4	0.5	100	35
	F-a 3	4	0.5	80	25
	F-a 4	4	0.5	60	15
F-b	F-b 1	4	1.0	120	45
	F-b 2	4	1.0	100	35
	F-b 3	4	1.0	80	25
	F-b 4	4	1.0	60	15
F-c	F-c 1	4	1.5	120	45
	F-c 2	3	1.5	120	45
	F-c 3	2	1.5	120	45
	F-c 4	1	1.5	120	45

The production process of thin plate specimen is shown in Figure 2. The specific production process is as follows:

- (1) Make a wood template, and reserve holes in the board for passing through the steel mesh.
- (2) Pass the steel strand through the hole reserved for the template, first through the longitudinal steel strand, and then through the horizontal steel strand, so that the vertical steel wires and the horizontal steel wires constitute the steel mesh.
- (3) Anchor both ends of the steel mesh to the side of the template with a lock.
- (4) Use a cross buckle to fix the wire mesh, and apply impermeable glue at the opening of the template extending out of the wire to prevent cement from flowing out.
- (5) Cut excess steel wire with steel wire pliers.
- (6) Prepare release agent with silica gel and talc powder, and brush release agent on the inner wall of the template to facilitate later release.
- (7) Take appropriate amount of polyisocyanate and polyol into the beaker and put it in 150° oven for 30 minutes. Polyurethane concrete is prepared according to the mix ratio and fully stirred to pour polyurethane concrete.
- (8) After the test piece was poured, the exposed cement surface is covered with plastic wrap. The formwork is removed 24 h later, and the test block was put into the standard curing room for curing. After the curing, the test piece is taken out of the standard curing room (temperature 20±2°C) for testing.

Experimental process

The loading of the bending test is shown in Figure 1. Switch the universal testing machine from tension mode to pressure mode, and install the support and loading head on the testing machine. Three displacement meters are arranged longitudinally at the mid-span of the thin plate specimen and under the loading head to measure the vertical deformation of the specimen. The displacement meter is arranged at the straddle and loading points respectively. The thin plate specimen is placed on the support, the upper and lower surfaces of the specimen are cleaned with alcohol, and the compressive strain and tensile strain are measured on the upper and lower surfaces as auxiliary test results. The load is measured in real time by a pressure sensor above the loading head. The test load is controlled by displacement, and the loading rate is constant at 0.5 mm/min. The test load and displacement meter data can be displayed on the computer in real time.

The test is carried out by four-point loading method. The distance between the two supports is 300 mm, the distance between the loading point and the support is 100 mm, and the distance between the loading point and the loading point is 100 mm.

After the test began, the traction loading head of the universal testing machine moved downward. When the loading head is in contact with the thin plate specimen, the load value and displacement value increase uniformly. As the test continued, the thin plate specimen gradually deformed, accompanied by the crisp fracture sound, a long crack appeared in the middle of the specimen, and the polyurethane cement was damaged. In the event of failure, the fracture of the steel strand and the cracking of the polyurethane cement occur almost simultaneously. At this time, the thin-plate specimen also reached the ultimate load and maximum deflection.



Fig. 1 - Four-point bending test

ANALYSIS OF FOUR POINT BENDING TEST RESULTS

Based on the pressure sensor and displacement meter, the load-mid-span displacement curve of the thin plate shaped SMPC specimen under the F-a specimen set is obtained, as shown in Figure 2. F-a1, F-a2, F-a3 and F-a4 have different specimen widths. The F-a1 specimen group with the smallest width but the largest reinforcement ratio has the largest average ultimate load of 13.85 kN. The F-a 4 specimen group with the largest width but the smallest reinforcement ratio has the smallest average ultimate load, which is 5.64 kN. With the increase of load, the mid-span displacement growth rate of F-a1 specimen group is significantly lower than that of the other three groups, which indicates that a higher width of specimen can significantly inhibit the expansion of mid-span displacement, but the width of specimen has almost no effect on the displacement growth.

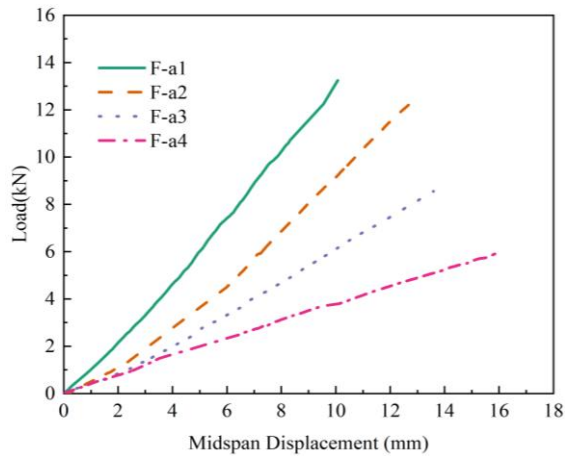


Fig. 2 - Load-displacement curve of F-a set

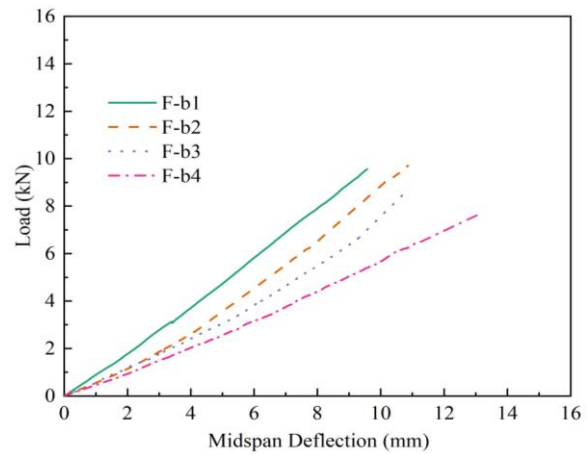


Fig. 3 - Load-displacement curve of F-b set

The load-displacement curve of the SMPC thin plate specimen of F-b specimen set is shown in Figure 3. Compared with the F-a set, the F-b set is made of polyurethane concrete with a rubber to powder ratio of 1. The F-b1 group with the largest width has the largest growth rate. The average limit load of group F-b1 can reach 9.72 kN, which is 29% larger than the 7.53 kN of group F-b4 respectively. In terms of mid-span displacement, F-b4 group has a maximum average mid-span displacement of 12.99 mm, which is 42 % higher than that of F-b1 group, which is 9.60 mm. In general, the ultimate load and the maximum mid-span displacement of each group in F-b set are lower than those in F-a set with rubber powder ratio of 1.5.

The load-displacement curve of the SMPC thin plate specimen of F-c specimen set is shown in Figure 4. F-c sets have steel mesh with different layers to explore the influence of reinforcement ratio on the bending properties of composites. In general, the ultimate load is positively correlated with the ratio of reinforcement, and the mid-span displacement is positively correlated with the ratio of reinforcement. According to the trend of the curve, the load-displacement curve of F-c1 group with the highest reinforcement ratio increases the fastest. When the ultimate load is reached, the average mid-span displacement of F-c1 group is 8.85 mm. F-c4 group has the slowest load growth among the four groups. When the load is 5.32 kN, the specimen breaks and fails. The F-c4 group with the smallest reinforcement ratio also has the largest mid-span displacement in this sample set, which is 11.66 mm.

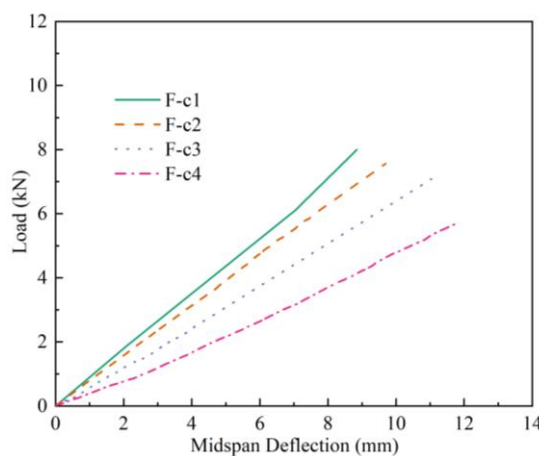


Fig. 4 - Load-displacement curve of F-c set

ANALYSIS OF INFLUENCE FACTORS

The width of the specimen significantly affects the maximum deflection and ultimate load of the SMPC specimen. F-a1, F-a2, F-a3 and F-a4 thin plate specimens have different widths, and the ultimate load values along the span direction of the specimens are shown in Figure 5. With the increase of the width of the specimen, the maximum deflection of the SMPC specimens also increases. The average maximum deflection of F-a4 specimen group is 15.85 mm, and the average maximum deflection is 1/20 of the span. The width of F-a1 specimen group is 120 mm, and the maximum bearing capacity is 13.85 kN. Compared with F-a2, F-a3 and F-a4 groups, the ultimate load of F-a1 is increased by 11%, 38% and 59%, respectively. This also shows that the increase of the width of the specimen increases the bending bearing capacity of the steel mesh reinforced polyurethane concrete (SMPC) material.

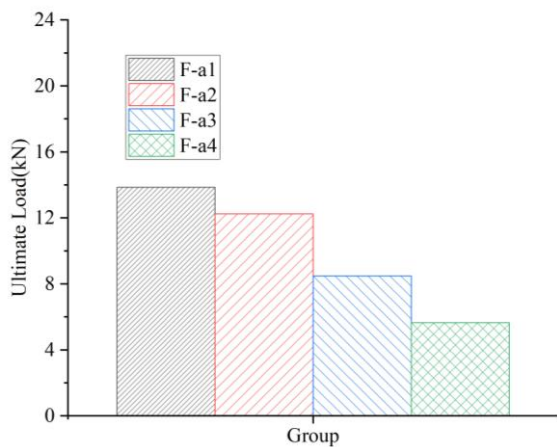


Fig. 5 - The influence of specimen width on the bending performance of composite materials

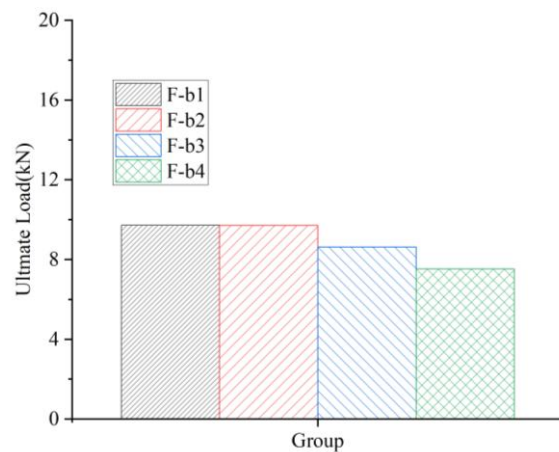


Fig. 6 - The influence of rubber powder ratio on the bending performance of composite materials

The ratio of glue to powder has a significant effect on the ultimate load of polyurethane concrete-steel mesh specimen, but has little effect on the maximum deflection. The relationship between the ultimate loads of thin plate specimens with different glue-powder ratios is shown in Figure 6. The maximum deflection of thin plate does not change significantly with the difference of PC mix ratio. The maximum deflection of F-a1, F-b1 and F-c1 specimens is 10.07 mm, 9.60 mm and 8.85 mm, respectively, with the maximum difference not exceeding 8%. The mix ratio of PC will affect the ultimate bending load. The F-a1 specimen with a glue-powder ratio of 1.5 is subjected to the maximum ultimate load, which is 30% and 42% higher than that of F-b1 specimen with a glue-powder ratio of 1.0 and F-c1 specimen with a glue-powder ratio of 0.5, respectively.

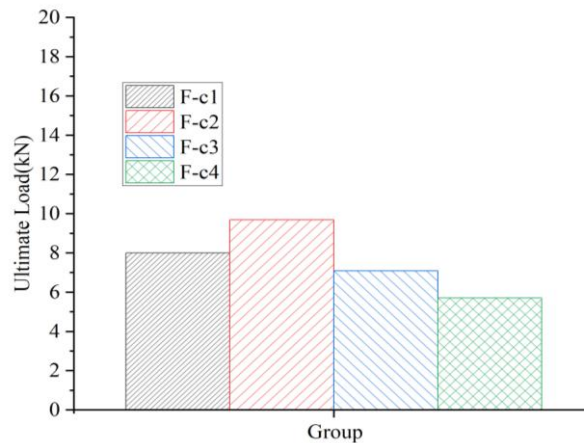


Fig. 7 - The influence of reinforcement ratio on the bending performance of composite materials

The reinforcement ratio can significantly affect the ultimate load and deflection of SMPC specimen. The relationship between reinforcement ratio of steel mesh and ultimate load at failure is shown in Figure 7. The ratio of reinforcement is negatively correlated with mid-span deflection. The average deflection of F-c1 specimen group with the largest reinforcement ratio is the smallest (8.85 mm). The mid-span deflection increases gradually with the decrease of steel mesh layers. The average deflection of F-c4 specimen group with the smallest reinforcement ratio is the largest, which is 11.66 mm. The ratio of reinforcement is positively correlated with the ultimate load. The ultimate load of F-c1 group with the highest reinforcement ratio is 8.0 kN, 17% lower than that of F-c2 group with a slightly smaller reinforcement ratio of 9.69 kN, 13% and 40% higher than that of F-c3 group and F-c4 group, respectively.

THEORETICAL ANALYSIS OF FOUR-POINT BENDING TEST

Calculation model of flexural capacity

(1) Tension model of high-strength steel mesh

The simplified stress-strain relationship of high-strength steel mesh is based on the double broken line model, as shown in Figure 8. The model simplifies the tension constitutive relation of steel strand into two stages. Its expression is shown in formula (1).

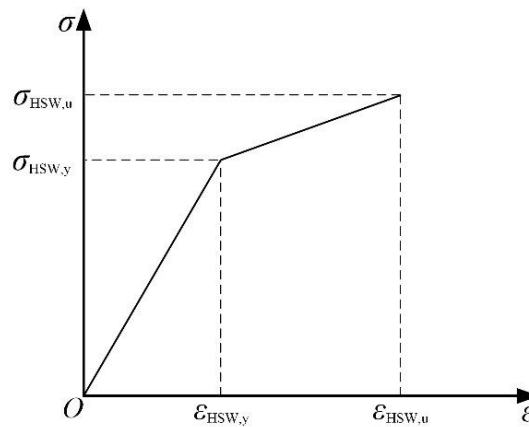


Fig. 8 - Simplified stress-strain relationship of tensile SM

$$\sigma_{SM} = \begin{cases} E_1 \varepsilon_{SM} & (0 \leq \varepsilon_{SM} \leq \varepsilon_{SM,y}) \\ \sigma_{SM,y} + E_2 (\varepsilon_{SM} - \varepsilon_{SM,y}) & (\varepsilon_{SM,y} \leq \varepsilon_{SM} \leq \varepsilon_{SM,u}) \end{cases} \quad (1)$$

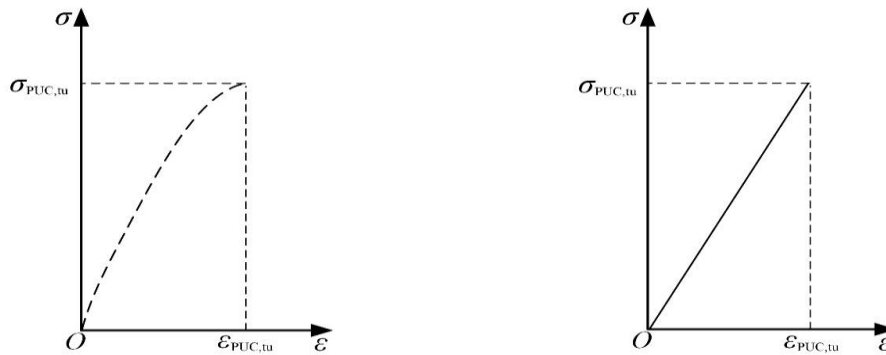
Where E_1 and E_2 are the elastic modulus of the mesh in the first and second stages respectively. The elastic modulus varies according to the diameter of the steel mesh, as shown in Table 2. $\sigma_{SM,y}$ is the tensile stress at the end of the first stage of the tensile process of the strand, and its value is about 80% of the ultimate tensile stress of the strand $\sigma_{SM,u}$. $\varepsilon_{SM,y}$ is the tensile strain at the end of the first stage in the tensile process of the steel mesh, and its value is about 45% of the ultimate tensile strain $\varepsilon_{SM,u}$.

Tab. 2 - Value of elastic modulus of F-c

Steel mesh layers	First stage elastic modulus E_1 (GPa)	Second stage elastic modulus E_2 (GPa)
1	135	32.0
2	130	31.5
3	108	22.5
4	97	21.3

(2) PC tensile model

The stress-strain simplified relationship of polyurethane concrete is shown in Figure 9. The constitutive relation of PC is simplified from quadratic function to linear relation. The simplified stress-strain curve is shown in Figure 10. $\sigma_{PC,tu}$ and $\varepsilon_{PC,tu}$ are the ultimate tensile stress and ultimate tensile strain of polyurethane concrete, respectively. The expression is shown in formula (2).



(a) Tensile constitutive relationship of PC

(b) Simplified tensile constitutive relationship of PC

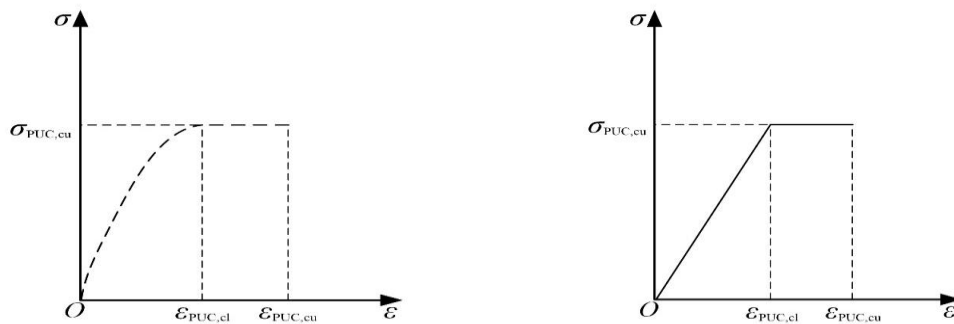
Fig. 9 - Stress-strain relationship of tensile PC

$$\sigma_{PC,t} = E_{PC,t} \varepsilon_{PC,t} \quad (2)$$

Where $\sigma_{PC,t}$ and $\varepsilon_{PC,t}$ are tensile stresses and strains of polyurethane concrete, respectively. $E_{PC,t}$ is the simplified tensile elastic modulus of polyurethane concrete, which is 4.5GPa.

(3) PC compression model

The compressive constitutive relationship of PC is shown in Figure 11. The nonlinear compression model is adopted. The model is similar to the stress-strain relationship in ECC, which is divided into ascending and flattening sections. In order to facilitate calculation, the compression model is also simplified, and the quadratic function relationship in the ascending section is simplified to a linear relationship. The simplified expression is shown in formula (3).



(a) Compressed constitutive relationship of PC

(b) Simplified compressed constitutive relationship of PC

Fig. 10 - Stress-strain relationship of compressed PC

$$\sigma_{PC,c} = \begin{cases} \frac{\varepsilon_{PC,c}}{\varepsilon_{PC,cl}} \sigma_{PC,cl} & (0 \leq \varepsilon_{PC,c} \leq \varepsilon_{PC,cl}) \\ \sigma_{PC,cu} & (\varepsilon_{PC,cl} \leq \varepsilon_{PC,cu}) \end{cases} \quad (3)$$

Where: $\sigma_{PC,c}$ is the compressive stress of polyurethane concrete, $\varepsilon_{PC,c1}$ is the compressive strain corresponding to the ultimate compressive strength of polyurethane concrete, $\varepsilon_{pc,c1}$ is the ultimate compressive strain at the top of the plate when the thin plate specimen is broken by bending, the ultimate compressive strain $\varepsilon_{PC,cu}$ is 0.02.

(4) Calculation formula of flexural bearing capacity

In the calculation of flexural strength of SMPC material, the working condition of SMPC material in tension area is considered. The stress-strain distribution of the section of thin plate specimen is shown in Figure 11. h and b represent the height and width of the specimen respectively. h_0 is the effective height of the section. a_s is the thickness of the protective layer of the steel mesh. x_0 is the height of compressive zone of PC. $\sigma_{hsw,t}$ and $\varepsilon_{hsw,t}$ are the stress and strain of high-strength steel mesh. $\sigma_{PC,t}$ and $\varepsilon_{PC,t}$ are tensile stresses and ultimate tensile stresses of PC, respectively. $\varepsilon_{PC,c}$ and $\varepsilon_{PC,u}$ are compressive strain and ultimate compressive strain of PC respectively. $\sigma_{PC,cu}$ is the ultimate compressive stress of polyurethane concrete. ψ is the tensile stress parameter of PC.

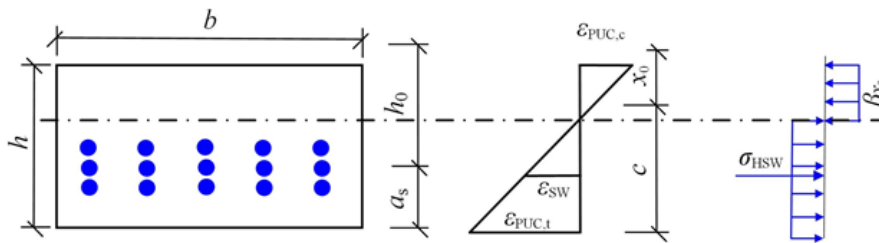


Fig. 11 - Stress and strain distribution of SMPC material during bending

According to the stress-strain distribution of the cross section of the composite material during bending, formula (4) is derived through the balance equation of force and bending moment:

$$M = \sigma_{SM} A_{SM} \left(h - a_s - \frac{1}{2} \beta x_0 \right) + \frac{1}{2} \sigma_{PC,t} b (h - x_0) [h + (1 - \beta) x_0] \quad (4)$$

Under the limit failure state of thin plate specimen, the strain and stress of high-strength steel mesh:

Where, b is the section width; h is the section height. For thin-plate specimens in this test, h is 25mm. σ_{SM} is the stress of steel mesh. a_{SM} is the height of the wire. For the thin plate specimen with the strand vertically centered, a_{SM} is 12.5mm. a_{SM} is the cross-sectional area of the longitudinal wire. The value is based on the diameter of the wire.

CONCLUSIONS

This paper presents a new material of steel mesh reinforced polyurethane concrete (SMPC). In order to verify the feasibility of this strengthening method, the mechanical properties of SMPC material are investigated by bending test of SMPC material sheet. The research conclusions are as follows:

(1) Increasing the width of thin plate specimens can improve the bending bearing capacity of steel mesh reinforced polyurethane concrete (SMPC) material. The width of the thin plate specimen

is 120 mm, and its maximum bearing capacity is 13.85 kN, and its ultimate load is 11%, 38% and 59% higher than that of the F-a2 (100 mm), F-a3 (80 mm) and F-a4 (60 mm) specimens, respectively. Maximum deflection reduced by 37%.

(2) The ratio of glue to powder has a significant effect on the ultimate load of SMPC specimen, but has little effect on the maximum deflection. The glue-powder ratio of F-a1 specimen group is 1.5 and the ultimate load is 13.85 kN, which is 42% and 73% higher than that of F-b1 specimen group with glue-powder ratio of 1.0 and F-c1 specimen group with glue-powder ratio of 0.5 respectively.

(3) The ultimate load of thin plate specimens increases with the increase of reinforcement ratio. The F-c1 specimen group exhibited the smallest mean deflection, only 8.85 mm, due to its highest reinforcement ratio. The ultimate load of F-c1 group with the highest reinforcement ratio reached 8.0 kN, which was 5.8% higher than that of F-c2 group with a slightly lower reinforcement ratio of 7.56 kN.

REFERENCES

- [1] Jiang Y., Yang G., Li H., 2023. Knowledge Driven Approach for Smart Bridge Maintenance Using Big Data Mining. *Automation in Construction*, vol. 146, pp. 104673. ISSN 0926-5805, <https://doi.org/10.1016/j.autcon.2022.104673>
- [2] Yanev B., Richardsl G. A. C., 2013. Designing Bridge Maintenance on the Network and Project Levels. *Structure and Infrastructure Engineering*, vol. 9, no. 4, pp. 349-363. ISSN 1573-2479, *Designing Bridge Maintenance on the Network and Project Levels*
- [3] Orcesi A. D., Frangopol D. M., Kim S., 2010. Optimization of Bridge Maintenance Strategies Based on Multiple Limit States and Monitoring. *Engineering Structures*, vol. 32, no. 3, pp. 627-640. ISSN 0141-02, <https://doi.org/10.1016/j.engstruct.2009.11.009>
- [4] Mahdi I M., Khalil A. H., Mahdi H. A., 2022. Decision Support System for Optimal Bridge' Maintenance. *International Journal of Construction Management*, vol. 22, no. 3, pp. 342-356. ISSN 1562-3599, <https://doi.org/10.1080/15623599.2019.1623991>
- [5] Ren G., Ding R., Li H., 2019. Building An Ontological Knowledgebase for Bridge Maintenance. *Advances in Engineering Software*, vol. 130, pp. 24-40. ISSN 0965-9978, <https://doi.org/10.1016/j.advengsoft.2019.02.001>
- [6] Furuta H., Kameda T., Nakahara K., 2006. Optimal Bridge Maintenance Planning Using Improved Multi-Objective Genetic Algorithm. *Structure and Infrastructure Engineering*, vol. 2, no. 1, pp. 33-41. ISSN 1573-2479, <https://doi.org/10.1080/15732470500031040>
- [7] Xing G., Wu T., Lliu B., 2010. Experimental investigation of Reinforced Concrete T-beams Strengthened with Steel Mesh Embedded in Polymer Mortar Overlay. *Advances in structural Engineering*, vol. 13, no. 1, pp. 69-79. ISSN 1369-4332, <https://doi.org/10.1080/15732470500031040>
- [8] Wang T., He M., Wu H., 2024. Experimental Study on RC Beams Shear-strengthened with Composite Polymer Mortar and Steel Strands Wire Mesh. *Structural Concrete*, vol. 25, no. 4, pp. 2660-2676. ISSN 1464-4177, <https://doi.org/10.1002/suco.202300630>
- [9] Siwowski T., Piatek B., Siwowska P., 2020. Development and Implementation of CFRP Post-tensioning System for Bridge Strengthening. *Engineering Structures*, vol. 207, pp. 110266. ISSN 0141-0296, <https://doi.org/10.1016/j.engstruct.2020.110266>
- [10] Sun L. P., Liu Z., Liu Y. Z., 2014. Analysis the Flexural Properties of RC Beams Strengthened by High Strength Steel Mesh and Polymer Mortar Using the Finite Element. *Applied Mechanics and Materials*, vol. 444, pp. 1067-1071. ISSN 1022-6680, <https://doi.org/10.4028/www.scientific.net/AMM.444-445.1067>
- [11] Li Y., Zhao S., Yao Z., 2023. Flexural Behavior of Reinforced Concrete Beams Strengthened Using Recycled Industrial Steel-wire Mesh High-performance Mortar. *Case Studies in Construction Materials*, vol. 19, pp. 02472. ISSN 2214-5095, <https://doi.org/10.1016/j.cscm.2023.e02472>

- [12] Liao W., Wang H., Li M., 2019. Large Scale Experimental Study on Bond Behavior Between Polymer Modified Cement Mortar Layer and Concrete. *Construction and Building Materials*, vol. 228, pp. 116751. ISSN 0950-0618, <https://doi.org/10.1016/j.conbuildmat.2019.116751>
- [13] Zhong S., He M., Ding, Y., 2023. Study on the Effect of Pre-stressed Level on the Force Performance of Wedge Steel Plate Jacket and Steel Mesh-PCM Strengthened RC Beams. *Structures*, vol. 57, pp. 105283. ISSN 2352-0124, <https://doi.org/10.1016/j.istruc.2023.105283>
- [14] Kexin Z., Qunsheng S. Strengthening of a Reinforced Concrete Bridge with Polyurethane-cement Composite (PUC). *The Open Civil Engineering Journal*, vol. 10, no. 1. ISSN 2164-3164, [https://doi.org/10.1061/\(ASCE\)CF.1943-5509.0001640](https://doi.org/10.1061/(ASCE)CF.1943-5509.0001640)
- [15] Hou N., Li J., Li X., 2022. Study on Toughening and Temperature Sensitivity of Polyurethane Concrete (PUC). *Materials*, vol. 15, no. 12, pp. 4318. ISSN 1996-1944, <https://doi.org/10.3390/ma15124318>
- [16] Zhang K., Zhu X., Cao Y., 2023. Experimental Study on Mechanical Properties of Polyurethane Concrete Composite (PUC) under Various Temperatures. *Materiale Plastice*, vol. 60, no. 2. ISSN 0025-5289, <https://doi.org/10.37358/Mat.Plast.1964>
- [17] Li C., Zhang W., Sun G., 2023. Research on Damping Properties and Microscopic Mechanism of Polyurethane Concrete-based Composites. *Construction and Building Materials*, vol. 365, pp. 130137. ISSN 0950-0618, <https://doi.org/10.1016/j.conbuildmat.2022.130137>
- [18] Zhang K., Sun Q., 2018. The Use of Wire Mesh-polyurethane Vement (WM-PUC) Composite to Strengthen RC T-beams Under Flexure. *Journal of Building Engineering*, vol. 15, pp. 122-136. ISSN 2352-7102, <https://doi.org/10.1016/j.jobe.2017.11.008>
- [19] Zhang K., Xuan J., Shen X., 2024. Investigating the Flexural Properties of Reinforced Concrete T-beams Strengthened with High-strength Steel Mesh and Polyurethane Concrete. *Journal of Bridge Engineering*, vol. 29, no. 5, pp. 04024023. ISSN 1084-0702, <https://doi.org/10.1061/JBENF2.BEENG-6524>